ЖЭТФ, 2010, том 137, вып. 1, стр. 136–148

BROKEN SPIN SYMMETRY APPROACH TO CHEMICAL REACTIVITY AND MAGNETISM OF GRAPHENIUM SPECIES

E. F. Sheka [a*], ***L. A. Chernozatonskii*** [b]

[a] *Peoples' Friendship University of the Russian Federation*
117923, Moscow, Russia

[b] *Emanuel Institute of Biochemical Physics, Russian Academy of Sciences*
119334, Moscow, Russia

Received June 1, 2009

The basic problem of weak interaction between odd electrons in graphene and silicene is considered in the framework of the broken spin symmetry approach. This approach exhibits the peculiarities of the odd-electron behavior via both enhanced chemical reactivity and magnetism.

1. INTRODUCTION

Odd electrons are a characteristic feature of the graphenium species. The term was introduced in organic chemistry in describing the electronic structure of diradicals and naturally covers the "π electrons", "magnetic electrons", and "dangling bonds" [1]. In the current case, the term indicates that the number of valence electrons in each carbon atom of graphene and carbon nanotubes (CNTs) as well as in each silicon atom of silicene and siliceous nanotubes (SiNTs) is larger by one than the number of interatomic bonds formed by the atom. Due to an increased length of the valence bonds of the species in comparison to the C–C bonds of a classic π-electron system of the benzene molecule, a considerable weakening of the electron interaction occurs, which causes a partial exclusion of odd electrons from the covalent bonding [2, 3], and hence the odd electrons covalently bound in the benzene molecule become effectively unpaired in graphenium species. These effectively unpaired electrons provide a radicalization of the species, which results in a considerable enhancement of their chemical reactivity and magnetism. They were once considered for carboneous and siliceous fullerenes [2, 4–6] and single-walled CNTs [3, 7]. In this paper, we address the problem in graphene and silicene.

A generalization of the quantum-chemical approach to systems with weakly interacting electrons ultimately requires taking the electron correlations into account and passing to computational schemes that involve the full configuration interaction. But the traditional complete active space self-consistent field (CASSCF) methods that deal correctly with two-electron systems of diradicals and some dinuclear magnetic complexes cannot handle systems with a large number of electrons due to a huge number of configurations generated in the active space of the system (for m singly occupied orbitals on each of the n identical centers, 2^{mn} Slater determinants should be formed by assigning spins up or down to each of the nm orbitals [8]). It has been assumed until recently that CASSCF-type approaches are nonfeasible for many-odd-electron systems such as fullerenes, CNTs, and graphene. Hence, resorting to single-determinant approaches appeared to be the only alternative.

The open-shell unrestricted broken spin symmetry (UBS) approach suggested in Ref. [9] is well elaborated for both wave-function and electron-density quantum-chemical methodologies, based on the unrestricted single-determinant Hartree–Fock scheme [10] (UBS HF) and the Kohn–Sham single Slater determinant procedure of the density functional theory (UBS DFT) [11]. The main problem in the UBS approach concerns spin contamination of the calculation results. The interpretation of UBS results in view of their relevance to the physical and chemical reality consists in mapping between the eigenvalues and eigenfunctions of the exact and model spin Hamiltonians. While the implementation of the UBS HF approach, both *ab initio*

*E-mail: sheka@icp.ac.ru

and semiempirical, is quite standard and the desired mapping is quite straightforward, this is not the case with the UBS DFT due to the total spin problem. As is known, the DFT cannot be directly applied to calculation of the spin and space multiplet structure, and a number of special procedures, all of which are beyond the pure DFT scope [12], are suggested to overcome this difficulty. The procedures differ in the computation schemes and in the obtained results, and therefore UBS DFT is theory-level dependent [12, 13].

Although the odd-electron problem seems to be obvious for benzenoid species, involving graphene and silicene in particular, the computational science of these carboneous nanomaterials has been restricted until now to the computational schemes (mainly DFT ones) based on the restricted approach. This implies that odd electrons are located on electron orbitals in pairs subordinating to the Pauli principle. Therefore, in the case where the odd-electron number is even, the ground state of the system is expected to be singlet, and hence the electron spins should not be taken into account. But for electrons that interact weakly, the restricted approach results in an unstable solution because there is another more stable unrestricted solution lower in energy (see a discussion of the problem in [9] and the references therein). It turns out that odd electrons are individually located on electron orbitals and the space orbitals for electrons with different spins are different. That is why the even-singlet state of the electron system becomes spin dependent while the total spin is equal to zero. These new features of the unrestricted solutions offer a large number of delicate characteristics that highlight new facets of the odd-electron behavior. In this paper, the first application of the unrestricted approach to graphene and silicene is given. A comparison of the results to findings obtained in the framework of many-body configuration interaction schemes [14, 15] manifests the UBS HF unique ability to quantitatively describe the practically important consequences of weak interaction between odd electrons of the studied nanospecies.

2. BASIC RELATIONS

2.1. Odd-electron-enhanced chemical reactivity

Weakly interacting odd electrons produce a number of effectively unpaired electrons, which in the framework of UBS solutions are directly related to the spin contamination

$$C = \langle \hat{S}^2 \rangle - S(S+1). \tag{1}$$

Here, $\langle \hat{S}^2 \rangle$ is the expectation value of the total spin angular momentum that follows from the UBS solution. The spin contamination C is tightly related to the Löwdin symmetry dilemma [16], which is expressed as asymmetric electron densities of the UBS HF solution and an asymmetric local spin density approximation (LSDA) Hamiltonian of UBS DFT with different exchange-correlation potentials for spin-up and spin-down orbitals. This feature exhibits the tendency of spin-up and spin-down electrons to occupy different portions of space. The asymmetry results in the appearance of the new density function first suggested by Takatsuka, Fueno, and Yamaguchi thirty years ago [17] and called the distribution of "odd" electrons,

$$D(r|r') = 2\rho(r|r') - \int \rho(r|r'')\rho(r''|r')\, dr'', \tag{2}$$

where ρ is the electron density. The trace of this function,

$$N_D = \operatorname{tr} D(r|r'), \tag{3}$$

was interpreted as the total number of such electrons. The authors suggested the function $D(r|r')$ to manifest the radical character of the species under investigation. 22 years later, Staroverov and Davidson changed the term to "distribution of effectively unpaired electrons" [18], emphasizing a radical character of taking N_D electrons out of the covalent bonding. It was suggested in [17] that the function $D(r|r')$ can be subjected to a population analysis in the framework of the Mulliken partitioning scheme, such that in the case of a single Slater determinant, Eq. (3) becomes [18]

$$N_D = \operatorname{tr} DS, \tag{4}$$

and

$$N_D = \sum_{i,j=1}^{NORBS} D_{ij}, \tag{5}$$

where

$$DS = 2PS - (PS)^2, \tag{6}$$

P is the density matrix, S is the orbital overlap matrix, and $NORBS$ is the number of orbitals. The effectively unpaired electrons that appear here point to the radicalization of the molecular species under study; their number is an evident quantifier of the radicalization or, in other words, of the enhanced chemical reactivity.

As shown in [18], the total number N_D of effectively unpaired electrons is related to spin contamination as

$$N_D = 2\left(\langle \hat{S}^2 \rangle - \frac{(N^\alpha - N^\beta)^2}{4}\right), \tag{7}$$

where N^α and N^β are the numbers of electrons with spin α and β. Therefore, quantifying N_D requires knowing either $\mathrm{tr}\, D(r|r')$ or $\langle\hat{S}^2\rangle$.

For a single-Slater-determinant UBS HF function, the evaluation of both quantities is straightforward because the corresponding coordinate wave functions are subordinated to the definite permutation symmetry, such that each spin value S corresponds to a definite expectation value of the energy [12]. Thus, $\langle\hat{S}^2\rangle$ is expressed as [19]

$$\langle S^2\rangle = \frac{(N^\alpha - N^\beta)^2}{4} + \frac{N^\alpha + N^\beta}{2} - \sum_{i,j=1}^{NORBS} P_{ij}^\alpha P_{ij}^\beta, \quad (8)$$

where $P_{ij}^{\alpha,\beta}$ are matrix elements of the electron density for spins α and β. Similarly, Eq. (5) has the form [5]

$$N_D = \sum_A^{NAT} N_{DA}, \quad (9)$$

where [5]

$$N_{DA} = \sum_{i\in \mathrm{A}} \sum_{B=1}^{NAT} \sum_{j\in \mathrm{B}} D_{ij}. \quad (10)$$

Here, D_{ij} are matrix elements of the spin density and NAT is the number of atoms. In the case of the neglecting-differential-double-overlapping approximation underlying the AM1/PM3 semiempirical computational schemes that we use below, this matrix is expressed as [5]

$$D = (P^\alpha - P^\beta)^2. \quad (11)$$

The N_{DA} value, attributed to the effectively unpaired electron number on atom A, is very important because it plays the role of the atomic chemical susceptibility. A correct determination of both N_D and N_{DA} is ensured by the AM1/PM3 UBS HF solution [5] of the CLUSTER-Z1 software [20] used in the current study.

Oppositely to UBS HF, UBS DFT faces a conceptual difficulty in the determination of both $\langle\hat{S}^2\rangle$ and $\mathrm{tr}\, D(r|r')$. This is due to the invariance of the electron density ρ under the permutation symmetry [12], with the result that DFT does not distinguish states with different spins. All attempts to include the total spin into consideration are related to either Ψ-based contributions to the DFT body or introducing the spin through exchange and correlation parts of functionals [12]. If spin-dependent exchange potentials can be presented analytically, there is no relation that connects the correlation potential with spin, and hence its spin dependence is completely arbitrary. That is why DFT relations similar to Eqs. (5)–(10) are absent, and every individual calculation of either $\langle\hat{S}^2\rangle$ or $\mathrm{tr}\, D(r|r')$ is of a partial interest and is related to a particular calculation scheme used in Refs. [21, 22].

2.2. Odd-electron magnetism

Magnetism of odd-electron systems, as the molecular magnetism, can be considered in terms of the Heisenberg Hamiltonian [23] involving the total spin and the exchange integral J (presently, often called the magnetic coupling constant [13]). The eigenfunctions of the Hamiltonian are simply spin eigenfunctions, and J is directly related to the energy difference corresponding to these eigenstates. The determination of the magnetic coupling constant is a central point of the magnetism study.

Many authors have attempted to apply the Heisenberg description of magnetic interaction to the electron structure of a molecular electron system (see reviews [13, 23] and the references therein). A successful description of such a delicate physical property lies in the appropriate mapping between the Heisenberg spin eigenstates and suitable computationally determined electron states. It is customary to derive a relation between J and the energy difference of pure spin states.

As regards the UBS HF approach, where electron states are definitely spin-mapped, the problem consists in the determination of pure spin states and the relevant J value from the spin-contaminated eigenvalues of the UBS HF solutions. The problem was perfectly solved by Noodleman [9, 23] within the broken spin symmetry approach. In the case of an even number of "magnetic" (odd) electrons, J is given by

$$J = \frac{E_{S=0}^{UBS\,HF} - E_{S_{max}}^{PS}}{S_{max}^2}, \quad (12)$$

where $E_{S=0}^{UBS\,HF}$ and $E_{S_{max}}^{PS}$ are the energies of the UBS HF singlet state and the pure spin state with the maximal spin S_{max}. This is an exact pure spin single-determinant solution. Consequently, the energy of the pure spin singlet state is determined by the equation [9]

$$E_{S=0}^{PS} = E_{S=0}^{UBS\,HF} + S_{max}J, \quad (13)$$

and the energy of the subsequent pure spin states of a higher spin multiplicity are given by

$$E_S^{PS} = E_{S=0}^{PS} - S(S+1)J. \quad (14)$$

As noted above, both the magnetic coupling constant J and pure spin states cannot be straightforwardly obtained in the DFT scope. Particular procedures are used to reach the goal. Without pretending

Table 1. Atomic chemical susceptibility of hydrogen-terminated nanographenes

NGr $(n_a, n_z)^*$	N_{DA}		
	Armchair edge	Central part	Zigzag edge
(15,12)	0.28–0.14	0.25–0.06	0.52–0.28
(15,12)**	1.18–0.75	0.25–0.08	1.56–0.93
(7,7)	0.27–0.18	0.24–0.12	0.41–0.28
(5,6)	0.27–0.16	0.23–0.08	0.51–0.21

*Following [32], n_a and n_z respectively match the numbers of benzenoid units on the armchair and zigzag ends of the sheets. **After removing the hydrogen terminators.

to give an exhaustive list of publications concerning the problem, we collect some representative examples in Refs. [24–29]. Some of these attempts are rather successful in terms of comparison with experimental data (this is the case with the long study of magnetic behavior of biomolecular complexes with transition metals [29]).

Magnetism is the phenomenon specified by weak electron interaction, i.e., a small absolute value of J. The smallness of J is particularly important for the occurrence of magnetism in systems with a singlet ground state due to the second-order character of the magnetic phenomenon in this case [30]. At the same time, the J value obviously correlates with the number of effectively unpaired electrons and the UBS spin density $D(r|r')$, which both increase as J decreases. However, there is no exact relation between J, on one hand, and either N_D or $D(r|r')$, on the other. That is why the empirically known upper limit of the absolute J value, at which the magnetization of a species occurs, at the level of 10^{-3}–10^{-2} kcal/mol [31], cannot be straightforwardly translated into the corresponding values for N_D or $D(r|r')$. Therefore, J remains the only quantity that may quantify the magnetic behavior from the theoretical standpoint.

3. CHEMICAL REACTIVITY OF GRAPHENE

Low and homogeneous chemical reactivity of inner atoms of a graphene sheet is usually expected by the predominant majority of scientists dealing with the graphene chemistry. But this is not the case because the length of equilibrium C–C bonds of graphene exceeds 1.395 Å, which is the upper limit of the complete covalent coupling between odd electrons [2, 3]. The calculated results for graphene sheets of different size (nanographens, NGrs) are listed in Table 1. We used rectangular NGrs labeled as (n_a, n_z) structures following [32]. Here, n_a and n_z respectively match the number of benzenoid units on the armchair and zigzag edges of the sheets. The atomic chemical susceptibility (N_{DA}) profile for NGr (15,12) with hydrogen-terminated edges presented in Fig. 1*a* demonstrates a rather significant variation of the quantity over atoms due to a noticeable dispersion of the C–C bond lengths. The bond dispersion occurs when equilibrating the starting configuration characterized by the constant C–C bond lengths of 1.42 Å over the sheet. As can be seen from the figure, the highest susceptibilities are characteristic of carbon atoms at the zigzag edges, and those of the armchair edges are similar to the values of the sheet inner atoms and are comparable with the ones of fullerenes [2, 5] and single-wall CNT sidewalls [3, 7].

When hydrogen terminators are removed, the N_{DA} profile over the sheet remains unchanged, while N_{DA} values on both zigzag and armchair edges increase significantly (Fig. 1*b*), still retaining bigger values for zigzag edges.

The obtained results allow drawing the following conclusions concerning the chemical reactivity of NGrs.

1. Any chemical addend is first attached to the NGr zigzag edges, both hydrogen terminated and empty.

2. Nonterminated armchair edges slightly different in activity complete with zigzag ones.

3. Chemical reactivity of inner atoms is independent of the edge termination and is comparable with that of single-wall CNT sidewalls and fullerenes, thus providing a large range of addition reactions at the NGr surface.

4. The disclosed chemical reactivity of both edges and inner NGr atoms causes a particular two-mode pattern (a normal mode and a tangent or parallel one) of the NGr attaching to any spatially extended molecular object such as a CNT or substrate surface.

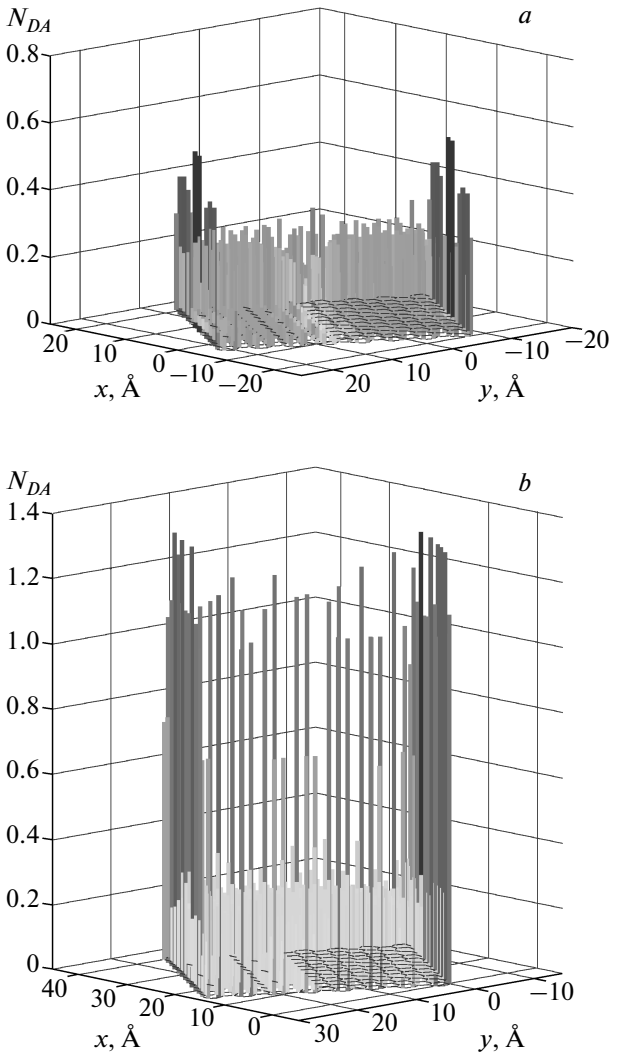

Fig. 1. Distribution of atomic chemical susceptibility (in electron units, e) over atoms of rectangular NGr(15,12) with hydrogen-terminated (a) and empty (b) edges. UBS HF solution. Singlet state

We consider the results of the UBS DFT studies of NGrs. The first notification about peculiar edge states of graphene ribbons appeared as early as 1987 [33], but further extended study started about ten years later [34, 35]. Since then, three main directions of the peculiarity investigation have formed, focused on 1) edge states within the band structure of graphene; 2) chemical reactivity, and 3) magnetism of graphene ribbon zigzag edges. The first topic mainly pertains to the solid state theory concerning the formation of localized states caused by the breakage of translational symmetry in a certain direction that occurs when a graphene sheet is cut into graphene ribbons. This fundamental property is well disclosed computationally independently of the technique used [35, 36] and has been confirmed experimentally [37, 38]. Two other topics are intimately connected with the UBS DFT [39–42] itself and demonstrate a spin-contaminated character of the obtained solutions.

The first UBS DFT examination of the chemical reaction between a hydrogen-terminated graphene ribbon and common radicals [39] disclosed unpaired π electrons (authors' nomenclature) distributed over zigzag edges in $0.14e$ on each atom (N_{DA} in the terminology of this paper). The finding permitted the authors to make conclusion about the open-shell character of the graphene singlet ground state of the ribbon and of the special chemical reactivity of the atoms that leads to partial radicalization of the species. The next authors' conclusion concerns nonedge ribbon carbon atoms, armchair atoms, and CNT (presumably, sidewall) atoms that show little or no radical character.

The cited UBS DFT results correlate with those of UBS HF of the current study in two aspects. Both approaches disclose the open-shell character of the ground singlet state of graphene and establish the availability of effectively unpaired electrons. But the numbers of effectively unpaired electrons differ by an order of magnitude, which restricted the UBS DFT discussion of the chemical reactivity of graphene to zigzag edge atoms only. The fixation of the open-shell character of the NGr singlet ground state by both UBS techniques is obvious due to the single-determinant character of the wave functions in the two cases. The feature is revealed due to considerable weakening of the odd-electron interaction in graphene caused by rather large C–C bond lengths. As regards the magnitude of the unpaired odd (π) electron numbers N_{DA}, it is difficult to discuss the corresponding DFT value because no indication of the way of its determination is presented. Its decrease by one order of magnitude compared to the UBS HF data might indicate a pressed-by-functional character of the UBS DFT calculations [13]. The functional-dependent character of the UBS DFT solutions was thoroughly analyzed just recently [43, 44]. At any rate, the results clearly exhibit a much lower sensitivity of the UBS DFT approach to the chemical reactivity of atoms, which can be imagined as lifting the zero reading level to $(0.2–0.3)e$ in Fig. 1a and to $1.1e$ in Fig. 1b, after which the fixation of values below the level becomes impossible.

The close-to-zero chemical reactivity of graphene inner atoms predicted by the UBS DFT calculations strongly contradicts the active chemical adsorption of individual hydrogen and carbon atoms on graphene surface recently found experimentally [45]. Gener-

ally, the chemical reactivity of inner atoms has been proven by the formation of a chemically bound interface between a graphene layer and silicon dioxide over the extent of the graphene sheet [46] and by producing a new particular one-atom-thick CH species called graphane [47]. At the same time, the empirical observations agree well with the UBS HF data obtained in this paper.

A strong support of the UBS HF data obtained can be found in the recent many-body configuration interaction calculations of polyacenes [14]. Applying *ab initio* density-matrix renormalization group (DMRG) algorithms, the authors highlighted the radical character of the acenes, which is caused by the appearance of effectively unpaired electrons and which starts in naphthalene and strengthens as the acene size increases, in full agreement with our UBS HF data for lower acenes found previously [3]. On the contrary, the UBS DFT approach rejects the radicalization in this case until the acene becomes quite long [48]. The DMRG approach also permitted determining the total number N_D of effectively unpaired electrons. In using the algorithm for the quantity determination suggested in [18] and presented in Eq. (5) in Sec. 2.1, the authors obtained N_D values that coincide with the relevant data obtained in the framework of the UBS HF approach based on the same algorithm [3], Table 2. The observed fitting of the DMRG and UBS HF approaches is undoubtedly a strong support of the ability of the UBS HF approach to highlight physical reality of a system of weakly interacting electrons. That is why we suppose that the obtained data on the chemical reactivity of graphene are quite reliable and the atomic chemical susceptibility values can serve as quantified pointers for predicting chemical reactions and/or modifications to which graphene can be subjected. Thus, the revealed reactivity of both NGr edge and inner atoms as well as a possible two-mode pattern of an NGr sheet approaching a CNT have allowed suggesting a number of peculiar graphene-nanotube composites [49, 50] whose appearance might be expected in the near future.

Table 2. The total number of effectively unpaired electrons in accordance with Eq. (5)

Molecule	N_D	
	UBS HF [3]	DMRG [14]
Benzene	0	–
Naphtalene	1.48	1.95
Anthracene	3.00	3.00
Tetracene	4.32	4.00
Pentacene	5.54	5.20

4. MAGNETISM OF ZIGZAG EDGED NANOGRAPHENES

The phenomenon, predicted and studied computationally for NGrs, is one of the hottest issues of the graphene science. At the heart of the statement of graphene magnetism are localized states whose flat bands are located in the vicinity of the Fermi level and whose peculiarities were attributed to zigzag edges [33–35, 40, 41, 43, 44]. In numerous UBS DFT studies, this fact was connected with the spin density on edge atoms. Computations were carried out in presumably Ψ-contaminated UBS DFT approximations in accordance with the following logical scheme: taking spins of edge atoms into account at the level of wave function; considering so-called antiferromagnetic (AFM) and ferromagnetic (FM) spin configurations with spin alignment up on one edge and down (up) on the other, or nonmagnetic configuration when up–down spin pairs are located at each edge; and performing calculations for these spin configurations. The obtained results have shown that 1) the AFM configuration corresponds to the open-shell singlet ground state and is followed in stability by FM and then nonmagnetic states; 2) the calculated spin density on edge atoms corresponds to the input spin configurations in all cases. It should be added that numerical results obtained in different studies differ from each other when different functionals are used in the calculations.

However, the UBS DFT AFM (singlet) state is as spin contaminated as the UBS HF state and the availability of the spin density is just a strong confirmation of the spin contamination. Nevertheless, the presence of spin density at zigzag edge atoms was accepted as a decisive point in heralding magnetism of graphene ribbons, after which the phenomenon was considered to be confirmed, which gave rise to strong optimism regarding a number of exciting possible applications of the material, in spintronics for example [51].

Because spin density is a direct evidence of the solution spin contamination, particularly for the singlet state, it is worth comparing spin density data computed at the UBS DFT and UBS HF levels of the theory. The UBS HF spin density distribution over NGr(15,12) atoms with hydrogen-terminated and empty edges is demonstrated in Fig. 2. As can be seen from the figure, the spin density is available at all atoms of the

Table 3. NGrs electronic characteristics*

NGrs**	The number of "magnetic" (odd) electrons	$E_{S=0}^{UBS\,HF}$, kcal/mol	J, kcal/mol	$E_{S=0}^{PS}$, kcal/mol	Singlet–triplet gap***, kcal/mol
(15,12)	400	1426.14	−0.42	1342.14	0.84
(7,7)	120	508.69	−1.35	427.69	2.70
(5,6)	78	341.01	−2.01	262.72	4.02

*The tabulated energies $E_{S=0}^{UBS\,HF}$ and $E_{S=0}^{PS}$ correspond to the heats of formation of the relevant states.
**For the nomenclature of nanographenes, see the footnote to Table 1.
***For pure spin states, the singlet–triplet gap $E_{S=1}^{PS} - E_{S=0}^{PS} = -2J$ [9].

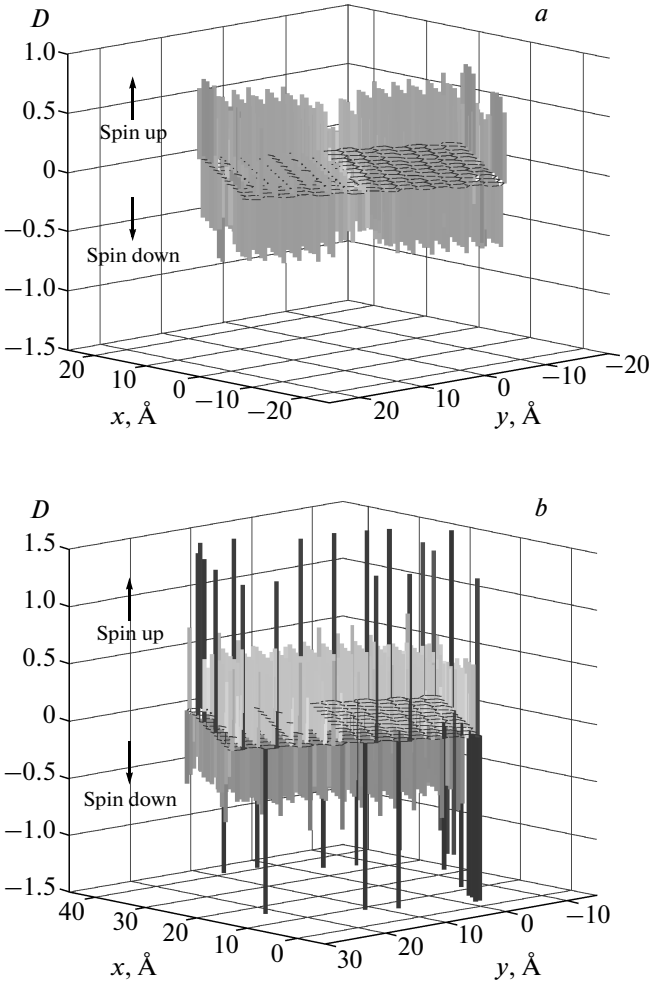

Fig. 2. Distribution of spin density (in electron units) over atoms of rectangular NGr(15,12) with hydrogen-terminated (a) and empty (b) edges. UBS HF solution. Singlet state

graphene sheet. In both cases, its summation over all atoms gives zero because a singlet state is considered. The spin density at zigzag edge atoms is the highest, even absolutely dominating when the edges are emptied. In contrast to this case, the UBS DFT data are related to zigzag edge atoms only and the absolute values of spin density vary from 0.26 to 0.47 when the local density functional is replaced by the screen exchange hybrid density functional [43]. To see only these atoms in Fig. 2 means shifting the zero reading level up (down) to about ±0.4 in the first case and to ±1.3 in the second case, which, in other words, means lowering the sensitivity in recording the density values. The same situation caused by the pressed-by-functional character of the UBS DFT solution was discussed for the N_{DA} profiles in the previous section.

We note that the UBS HF spin density on a zigzag edge is distributed quite peculiarly, not following the above-mentioned up- and down-edge AFM regular configuration assumed for the ground state by UBS DFT. Recalling that the spin density value is sensitive to the C–C bond length, it becomes clear why varying that length produces variation in the density distribution as well. Therefore, the UBS HF data differ from those of UBS DFT both qualitatively and quantitatively, not supporting a ranged configuration of spins on zigzag edge atoms only. At the same time, the UBS HF data well correlate with (presently, the only) many-body configuration interaction calculations of the edge states of graphene [15]. It follows from these calculations that although the electrons have the tendency to accumulate at the edges, their spins are distributed without order, and hence a regular net spin polarization of the edges is highly improbable. Therefore, as in the case of the chemical reactivity of graphene discussed in the previous section, many-body configuration interaction calculations are well correlated with UBS HF ones, thus

supporting the ability of the approach to highlight the main physical features of weakly interacting electrons.

Returning to magnetism of graphene ribbons, we have to proceed from the fact that the real ground state of the object is a pure spin singlet. This means that the real spin density at each atom is zero. We can nevertheless discuss the possibility of the magnetic behavior of the object, although not from the spin density standpoint but addressing the energy difference between states of different spin multiplicities as was discussed in Sec. 2.2.

An attempt to go beyond the spin-density concept at the UBS DFT level was made just recently [43]. This time, the main attention was focused on the difference in position of the singlet and higher-spin (mainly, triplet) states of NGrs, thus implicitly appealing to the J value. However, as noted in Sec. 2.2, the magnetic coupling constant J should be attributed to the difference of pure spin states, while the UBS DFT states under discussion are spin-mixed, and their energies do not therefore correspond to those of pure spin states, which makes the conclusions in [43] quite uncertain.

In contrast to UBS DFT, the UBS HF offers a straightforward way to determine pure spin states [9]. Computed in accordance with Eqs. (12)–(14), the $E^{PS}_{S=0}$, $E^{UBS\,HF}_{S=0}$, and J values related to the studied NGrs are listed in Table 3. As can be seen from the table, the ground state of all species is singlet, and hence a question arises as to whether the magnetization of a singlet-ground-state object is possible. As discussed in [30], the phenomenon may occur as a consequence of mixing the state with a higher-multiplicity one, e.g., in accordance with the van Fleck mixing promoted by an applied magnetic field [52]. Because the effect appears in the first-order perturbation theory, it depends on J, which determines the energy differences in denominators. Consequently, J should be small to provide a noticeable magnetization. Obviously, the singlet–triplet mixing is the most influent. As follows from Table 3, the energy gap to the nearest triplet state for the studied NGrs constitutes 1–4 kcal/mol. The value is large to provide a noticeable magnetization of these molecular magnets [31]. However, the value gradually decreases as the number of odd electrons increases. The behavior is similar to that obtained for fullerene oligomers [6], which led to the suggestion of a scaling mechanism of the nanostructured solid state magnetism of polymerized fullerene C_{60}.

In view of this idea, we estimate how large NGr should be to provide a noticeable magnetization. As mentioned in [31], molecular magnetism can be fixed at the J value 10^{-3}–10^{-2} kcal/mol or less. Based on the data in Table 3 and assuming the quantity to be inversely proportional to the number of odd electrons, we obtain $N \sim 10^5$. In NGrs, N coincides with the number of carbon atoms, which is determined for rectangular NGrs as [32]

$$N = 2(n_a n_z + n_a + n_z), \tag{15}$$

where n_a and n_z are the respective numbers of benzenoid units on the armchair and zigzag ends of the sheets. To fit the needed N value, the indices n_a and n_z should be given by a few hundreds, which leads to linear sizes of the NGrs equal to a few nanometers. The estimation is rather approximate, but it nevertheless correlates well with experimental observations of the magnetization of activated carbon fibers consisting of nanographite domains nearly 2 nm in size [53, 54].

The obtained results highlight another important aspect of the graphene magnetism exhibiting the relation of the phenomenon to a particular nanosize effect. This means that the graphene magnetization is observed for nanosize samples only, moreover, for samples whose size is within a particular interval, while the phenomenon does not occur in either very small or macroscopically large samples. Photoluminescence of nanosize silicon crystals [55] and other semiconductive grains [56] can be the best examples of such phenomena. Actually, an individual benzenoid unit (including a benzene molecule) is nonmagnetic (only slightly diamagnetic). When the units are joined to form a graphene-like cluster, effectively unpaired electrons appear due to weakening the interaction between odd electrons. The weakening accelerates as the cluster size increases, which is followed by a decrease in the magnetic constant J until it achieves a critical level that provides a noticeable mixing of the singlet ground state with higher-level spin states for the cluster magnetization to be fixed. And as long as the increase in the cluster size does not violate the molecular cluster-like behavior of odd electrons, the cluster magnetization increases. But as soon as the electron behavior becomes spatially quantizied, the molecular character of the magnetization is broken and substituted by that determined by the electron band structure based on the properties of a unit cell. A joint unit cell of graphene involves two atoms that form one C–C bond of the benzenoid unit; that is why we return to the case of a large magnetic constant J when the magnetization becomes nonobservable. A similar situation occurs in the case of polymerized C_{60}-fullerene crystals. The crystal unit cells involve either one (tetragonal and orthorhombic) or two (hexagonal) diamagnetic molecules, and hence the cell magnetic constant is either J or $J/2$, both

large, which does not allow fixing the magnetization of a perfect crystal. On the other hand, when the crystal is nanostructured by producing nanosize scales, the molecular-like behavior of odd electrons of the clusters provides a significant weakening of the interaction between them, which gives rise to small J and to cluster magnetization [6]. In both cases, the critical cluster size is given by a few nanometers, to be compared with the electron mean free path l_{el}. Evidently, when the cluster size exceeds l_{el}, the spatial quantization quenches the cluster magnetization. An accurate determination of l_{el} for odd electrons in graphene is not known, but the analysis of a standard database for the electron mean free paths in solids [57] shows that the quantity should be in the vicinity of 10 nm, which is supported by experimental data of a 3–7 nm electron free path in thin Cu-phthalocyanine films [58].

5. SILICEOUS GRAPHENE–SILICENE

A comparative study of carboneous and siliceous counterparts has always been one of hottest topics in material science and chemistry. The current interest in the subject has been stimulated by extreme expectations related to graphenium nanoprocessors. However, despite the reigning optimism about the devices, the graphene discoverers pointed out that the processors are unlikely to appear in the next 20 years [59] because replacement of the current silicon electronics technology is an extremely complicated issue. On the other hand, a compatibility of silicon-based nanoelectronics with the conventional one has enhanced attention to the question whether carboneous graphene can be substituted by its siliceous counterpart. Meeting the demands, the December '08 internet news reported on "epitaxial growth of graphene-like silicon nanoribbons" [60]. The report, based on the hexagon-patterned accommodation of silicon atoms adsorbed on the [110] Ag surface, has heralded the silicene manifestation and is full of exciting potential applications.

However, under detailed examination, the situation does not seem so transparent and promising. To clarify this, we specify basic terms. First, we make clear what is implied under the term "silicene". If any hexagon-packed structure of silicon atoms can be named silicene, then it has been known since as long ago as, say, the widely known silicon nanowires. However, four valence electrons of each silicon atoms form the sp^3 configuration and participate in the formation of four chemical bonds in this case, and hence nobody could pretend to have observed a similarity between these species and carboneous graphene. Therefore, not the hexagon packing itself but a mono-atom-thick hexagon structure that dictates the sp^2 configuration for atom valence electrons with the lack of one neighbor for each silicon atom meets the requirements of comparison of silicene to graphene. Obviously, similar hexagon patterns should form the ground for silicon nanotubes (SiNTs). Only under these conditions can graphene and silicene, as well as CNTs and SiNts, be considered on the same basis.

As regards theoretical analysis, the performed computations of silicene [61] and SiNTs [62–64] meet the requirement completely. On the other hand, experimental reports frequently refer to SiNTs (see brief review [65]) and silicene [60] (in the first announcement of the finding observed [66], it was attributed to silicon nanowires) in spite of the evident sp^3 configuration of silicon atoms in the structures observed. The fact was accepted by the experimentalists themselves. But a temptation to disclose SiNts and silicene seems to be so strong that the difference in the electron configuration is simply ignored. A detailed analysis of the available experimental data shows that silicon structures that can be compared to CNTs and graphene have not yet been observed. If we recall that fullerene Si_{60} has not been produced either, we have to accept the existence of a serious reason for such a drastic difference between carboneous and siliceous analogues.

The problem is not new and is rooted deeply: "... A comparison of the chemistry of tetravalent carbon and silicon reveals such gross differences that the pitfalls of casual analogies should be apparent" [67]. Suffice it to mention that there are neither silicoethylene nor silicobenzene, nor other silico-aromatic molecules. A widely spread standard statement that "silicon does not like the sp^2 configuration" just postulates the fact but does not explain the reason of such behavior. A real reason was disclosed for the first time when answering question why fullerene Si_{60} does not exist [4, 68]. The answer addresses changes in the electron interaction for the two species when their electron configurations are transformed from the sp^3 to the sp^2 type. The interaction of two odd electrons formed under the sp^3-to-sp^2 transformation of any interatomic bond depends on the corresponding distance R_{int}, which is about 1.5 times larger for Si–Si chemical bonds than for the C–C ones. As was shown, generally, the distance $R_{int} = 1.395$ Å is critical for these electrons to be covalently coupled [2]. Above this distance, the electrons become effectively unpaired, the stronger the larger the distance. In the case of graphene, the distances between two odd elect-

Table 4. Energies* and the number of effectively unpaired electrons in sp^2-configured siliceous species (see Fig. 3)

Species	N (N_2)**	$E_{S=0}^{RHF}$, kcal/mol	$E_{S=0}^{UBS\,HF}$, kcal/mol	$E_{S=0}^{PS}$, kcal/mol	N_D
I	2	54.50	48.95	39.02	0.88
II	6	144.51	121.25	108.67	2.68
III	60	1295.99	1013.30	996.64	62.48
IVa	96 (24)	2530.19	1770.91	1749.56	128
IVb	96	1943.14	1527.77	1505.48	95.7
Va	100 (20)	2827.73	1973.67	1958.54	115.05
Vb	100	2119.60	1580.77	1559.64	100.12
VIa	60 (22)	1950.20	1359.44	1346.68	75.7
VIb	60	1253.39	1001.27	972.12	54.04

*The tabulated energies $E_{S=0}^{RHF}$, $E_{S=0}^{UBS\,HF}$, and $E_{S=0}^{PS}$ and correspond to the heats of formation of the relevant states.
**Numbers in parentheses are N_2 of two-neighbor edge silicon atoms.

rons fill the interval 1.39–1.43 Å. Evidently, only parts of C–C bonds exceed the limit value, which causes partial exclusion of odd electrons from the covalent coupling and makes the molecular species partially radicalized as discussed in Sec. 2. The radicalization is rather weak because only nearly 20 % of all odd electrons (equal to the number of atoms N) are unpaired. But R_{int} in siliceous species is equal to 2.3–2.4 Å, which causes a complete unpairing of all odd electrons, and hence all siliceous species with the expected sp^2 configuration should be many-fold radicals.

The application of the UBS HF approach to the problem makes these expectations evident. Table 4 lists calculation results of the total number of unpaired electrons N_D and a set of energetic parameters for a number of siliceous sp^2-configured species shown in Fig. 3. As can be seen from the table, there is a drastic decrease in the total energy of the species, amounting to about 20–30 % of the largest values, when the close-shell restricted HF scheme is substituted by the open-shell UBS HF. Large N_D numbers of effectively unpaired electrons [2] for all species indicate a highly spin-contaminated character of their singlet UBS HF state. Following the procedure suggested in [9], we were able to determine the energy of the singlet pure spin states in accordance with Eq. (13). The energies $E_{S=0}^{PS}$ thus obtained are given in Table 4. As could be expected, the energy is lower than both $E_{S=0}^{RHF}$ and $E_{S=0}^{PS\,HF}$, while rather close to the latter.

We emphasize that the numbers of effectively unpaired electrons N_D listed in the table coincide quite well with the total numbers N of silicon atoms in all cases where the edges of the considered siliceous species are terminated by hydrogen atoms and exceed N by the number of two-neighbor atoms (N_2) when hydrogen terminators are removed from either tube ends or silicene edges. The finding exhibits that silicon fullerene as well as SiNTs, and silicene are many-fold radicals and cannot exist under ambient conditions. Importantly, no suitable passivation should be expected to provide the species stabilization because the passivation should be absolutely total, which would result in the transformation of all sp^2-silicon atoms into sp^3-ones. That is why sp^3-silicon nanowires are observed instead of sp^2-SiNTs [65] and sp^3-accommodated silicon atom adsorption layers on the (111) Ag surface are observed instead of sp^2-silicene strips [60, 66].

The optimism expressed in theoretical papers where fullerene Si_{60} [69], SiNts [62–64], and silicene [61] were considered is mainly because the calculations were performed in the close-shell approximation (similar to the restricted HF) and therefore the problem of weakly interacting odd electrons was not taken into account.

6. CONCLUSION

The basic problem of weak interaction between odd electrons in graphenium species is considered in the framework of the broken spin symmetry single-determinant approach. The modern implementations of the approach in the form of either the unrestricted Hartree–Fock scheme (UBS HF) or spin-polarized DFT (UBS DFT) were discussed with the emphasis on the

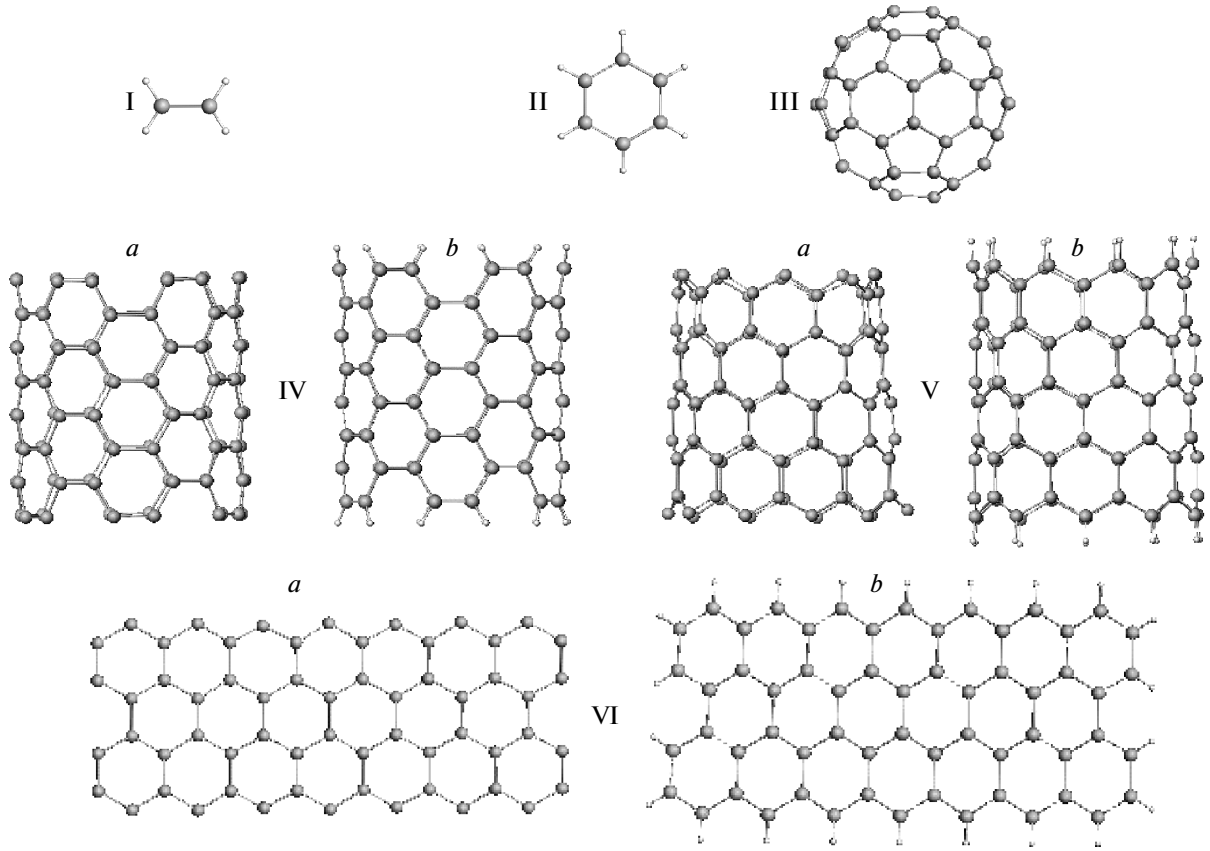

Fig. 3. Equilibrated structures of sp^2-configured siliceous species, UBS HF, singlet state: I — silicoethylene; II — silicobenzene; III — silicofullerene Si_{60}; IV — fragments of (6,6) SiNT with empty (a) and hydrogen-terminated (b) end atoms; V — the same for (10,0) SiNT; VI — (3,7) silicene sheet with empty (a) and hydrogen-terminated (b) edges

applicability of spin-contaminated solutions of both techniques to the description of electronic properties of the species. For graphene, the UBS DFT applications generally reveal the open-shell character of the singlet state of the object and manifest an extra spin density concentrated on zigzag edge atoms. Similarly, our study shows that the UBS HF approach supports these findings but exhibits the extra spin density not only on zigzag edge atoms but also on all atoms of the sheet. This peculiarity permits quantitatively describing the odd-electron behavior via both enhanced chemical reactivity and magnetism. The former is presented in terms of a quantified atomic chemical susceptibility that is continuously distributed over all nonedge inner atoms with the value similar to that for fullerenes and CNTs sidewalls and is twice or five times greater on zigzag edge atoms depending on whether those are terminated (by hydrogen) or empty. The armchair edge atoms four times prevail over the inner ones only in the absence of chemical termination.

Magnetic response of graphene sheets is shown to be provided by a collective action of all odd electrons and to be molecular-like by nature, which attributes the phenomenon to the size effect. The relative magnetic coupling constant J decreases as the sheet size increases and J approaches the limit value 10^{-3}–10^{-2} kcal/mol needed for the object magnetization to be recorded, when the sheet is a few nanometers in size, which is consistent with experimental findings. When the linear size exceeds the mean free path of odd electrons and spatial quantization of the odd electron behavior occurs, the magnetization becomes nonobservable due to a large value of the magnetic coupling constant J determined by the electron interaction within a unit cell containing two carbon atoms.

The explanation suggested by the UBS HF approach seems quite reasonable. A common view on both chemical reactivity and magnetism of graphene, physically clear and transparent, witnesses the internal consistency of the approach and exhibits its

high ability to quantitatively describe practically important consequences of weak interaction between odd electrons. The statement is well supported by a deep coherency of the obtained UBS HF results with those following from the application of many-body configuration interaction calculation schemes to polyacenes and graphene. Applied to silicene, the approach reveals a complete unpairing of odd electrons of the species, which transforms it into many-fold radicals and makes the substance absolutely impossible to produce.

This work was supported by the RFBR (grant № 08-02-01096).

REFERENCES

1. E. F. Sheka, Int. J. Quant. Chem. **107**, 2932 (2007).
2. E. F. Sheka, Int. J. Quant. Chem. **107**, 2803 (2007).
3. E. F. Sheka and L. A. Chernozatonskii, J. Phys. Chem. C **111**, 10771 (2007).
4. E. F. Sheka, Int. J. Quant. Chem. **100**, 388 (2004).
5. E. F. Sheka and V. A. Zayets, Zh. Fiz. Khimii **79**, 2250 (2005).
6. E. F. Sheka, V. A. Zayets, and I. Ya. Ginzburg, Zh. Eksp. Teor. Fiz. **130**, 840 (2006).
7. E. F. Sheka and L. A. Chernozatonskii, Int. J. Quant. Chem. **110** (2010), DOI:10.102/qua.22286.
8. E. R. Davidson and A. E. Clark, Phys. Chem. Chem. Phys. **9**, 1881 (2007).
9. L. Noodleman, J. Chem. Phys. **74**, 5737 (1981).
10. J. A. Pople and R. K. Nesbet, J. Chem. Phys. **22**, 571 (1954).
11. U. von Barth and L. Hedin, J. Phys. C **5**, 1629 (1972).
12. I. Kaplan, Int. J. Quant. Chem. **107**, 2595 (2007).
13. C. Adamo, V. Barone, A. Bencini et al. J. Chem. Phys. **124**, 107101 (2006).
14. J. Hachmann, J. J. Dorando, M. Aviles, and G. K. Chan, J. Chem. Phys. **127**, 134309 (2007).
15. S. Dutta, S. Lakshmi, and S. K. Pati, Phys. Rev. B **77**, 073412 (2008).
16. P. O. Löwdin, Adv. Chem. Phys. **14**, 283 (1969).
17. K. Takatsuka, T. Fueno, and K. Yamaguchi, Theor. Chim. Acta **48**, 175 (1978).
18. V. N. Staroverov and E. R. Davidson, Chem. Phys. Lett. **330**, 161 (2000).
19. D. A. Zhogolev and V. B. Volkov, *Methods, Algorithms, and Programs for Quantum-Chemical Calculations of Molecules* (in Russian), Nauk. Dumka, Kiev (1976).
20. V. A. Zayets, *CLUSTER-Z1: Quantum-Chemical Software for Calculations in the s,p-Basis* (in Russian), Institute of Surface Chemistry, Nat. Ac. Sci. of Ukraine, Kiev (1990).
21. J. Wang, A. D. Becke, and V. H. Smith, Jr. J. Chem. Phys. **102**, 3477 (1995).
22. A. Cohen, D. J. Tozer, and N. C. Handy, J. Chem. Phys. **126**, 214104 (2007).
23. L. Noodleman and E. Davidson, Chem. Phys. **109**, 1311 (986).
24. J. Schnack, Lect. Notes Phys. **645**, 155 (2004).
25. F. Illas, I. de P. R. Moreira, C. de Graaf, and V. Barone, Theor. Chem. Account **104**, 265 (2000).
26. H. Nagao, M. Nishino, Y. Shigeta et al., Coord. Chem. Rev. **198**, 265 (2000).
27. D. Dai and M.-H. Whangbo, J. Chem. Phys. **114**, 2887 (2001).
28. D.-K. Seo, J. Chem. Phys. **127**, 184103 (2007).
29. W.-C. Han and L. Noodelman, Inorg. Chim. Acta **361**, 973 (2008).
30. A. K. Zvezdin, V. M. Matveev, A. A. Mukhin et al., *Rear Earth Ions in Magnetically Ordered Crystals* (in Russian), Nauka, Moscow (1985).
31. O. Kahn, *Molecular Magnetism*, VCH, New York (1993).
32. X. Gao, Z. Zhou, Y. Zhao, S. Nagase, S. B. Zhang, and Z. Chen, J. Phys. Chem. A **112**, 12677 (2008).
33. S. E. Stein and R. L. Brown, J. Amer. Chem. Soc. **109**, 3721 (1987).
34. M. Fujita, K. Wakabayashi, K. Nakada, and K. Kusakabe, Phys. Soc. Jpn. **65**, 1920 (1996).
35. K. Nakada, M. Fujita, G. Dresselhaus, and M. S. Dresselhaus, Phys. Rev. B **54**, 17954 (1996).
36. Y. Miyamoto, K. Nakada, and M. Fujita, Phys. Rev. B **59**, 9858 (1999).
37. Y. Kobayashi, K. Fukui, T. Enoki et al., Phys. Rev. B **71**, 193406 (2005).

38. Y. Niimi, T. Matsui, H. Kambara et al., Phys. Rev. B **73**, 085421 (2006).

39. D. Jiang, B. G. Sumper, and S. Dai, J. Chem. Phys. **126**, 134701 (2007).

40. Z. Chen, D. Jiang, X. Lu et al., Org. Lett. **9**, 5449 (2007).

41. H. Lee, Y.-W. Son, N. Park et al., Phys. Rev. B **72**, 174431 (2005).

42. D. Jiang, B. G. Sumper, and S. Dai, J. Chem. Phys. **127**, 124703 (2007).

43. O. Hod, V. Barone, and G. E. Scuseria, Phys. Rev. B **77**, 035411 (2008).

44. S. Dutta and S. K. Pati, J. Phys. Chem. B **112**, 1333 (2008).

45. J. C. Meyer, C. O. Girit, N. F. Crommie, and A. Zettl, Nature **454**, 319 (2008).

46. Ph. Shemella and S. Nayak, Appl. Phys. Lett. **94**, 032101 (2009).

47. D. C. Elias, R. R. Nair, T. M. G. Mohiuddin et al., Science **323**, 610 (2009).

48. J. Poater, J. M. Bofill, P. Alemany, and M. Sola, J. Phys. Chem. A **109**, 10629 (2005).

49. E. F. Sheka and L. A. Chernozatonskii, arXiv:0901.3624v1.

50. E. F. Sheka and L. A. Chernozatonskii, Pis'ma v Zh. Eksp. Teor. Fiz. **89**, 412 (2009).

51. Y.-W. Son, M. L. Cohen, and S. G. Louie, Nature **444**, 347 (2006).

52. J. H. Van Fleck, *The Theory of Electric and Magnetic Susceptibilities*, Oxford (1932).

53. Y. Shibayama, H. Sato, T. Enoki, and M. Endo, Phys. Rev. Lett. **84**, 1744 (2000).

54. T. Enoki and Y. Kobayashi, J. Matter. Chem. **15**, 3999 (2005).

55. L. Khryachtchev, S. Novikov, and J. Lahtinen, J. Appl. Phys. **92**, 5856 (2009).

56. A. L. Sroyuk, A. I. Kryukov, S. Ya. Kuchmij, and V. D. Pokhodenko, Teor. Eksp. Khimia **41**, 67 (2005).

57. M. P. Seach and W. A. Dench, Surf. Interf. Analysis **1**, 2 (2004).

58. S. A. Komolov, E. F. Lazneva, and A. S. Komolov, Pis'ma v Zh. Tekhn. Fiz. **29**, 13 (2003).

59. A. K. Geim and K. S. Novoselov, Nature Materials **6**, 183 (2007).

60. A. Kara, C. Leandri, M. E. Davila et al., arXiv:0811.2611v1.

61. G. G. Guzman-Verri and L. C. Lew Yan Voon, Phys. Rev. B **76**, 075131 (2007).

62. S. B. Fagan, R. J. Baierle, R. Mota et al., Phys. Rev. B **61**, 9994 (2000).

63. R. Q. Zhang, S. T. Lee, C.-K. Law et al., Chem. Phys. Lett. **364**, 251 (2002).

64. B. Yan, G. Zhou, J. Wu et al., Phys. Rev. B **73**, 155432 (2006).

65. D. Perepichka and F. Rosei, Small **2**, 22 (2006).

66. P. de Padova, C. Quaresima, P. Perfetti et al., Nano Lett. **8**, 271 (2008).

67. P. Gaspar and B. J. Herold, in *Carbene Chemistry*, ed. by W. Kirsme, Acad. Press, New York (1971), Ch. 13, p. 504.

68. E. F. Sheka, in *Lecture Notes in Computer Science, Computational Science — ICCS2003*, Pt. II, ed. by P. M. A. Sloot, D. Abramson, A. V. Bogdanov, J. Dongarra, A. Y. Zomaya, and Y. E. Gorbachev, Springer, Berlin (2003), p. 386.

69. L. Bao-xing, C. Pei-lin, and Q. Duan-lin, Phys. Rev. B **61**, 1685 (2000).